

Chapter 2

Bose-Einstein condensation

Bose-Einstein condensation (BEC) has proved an astonishingly rich research topic, with many exciting developments including atom lasers [13, 87], vortices [88, 89] and vortex lattices [90], condensate collapse [14], and the observation of degeneracy in a Fermi gas [3]. Quantum degenerate mixtures of two or more atomic species exhibit a still wider range of phenomena, some of which have already been mentioned in the introduction to this thesis. However, the experimental potential of such systems is still largely unexplored. This chapter is intended to give an overview of the physics of Bose-Einstein condensation and low-temperature scattering theory, with an emphasis on how these may be applied to the study of mixtures of two different bosonic species.

2.1 What is a BEC?

Let us consider a system of N identical bosons with a temperature T and chemical potential μ . For the moment, we will ignore interactions between the bosons. The Bose-Einstein energy distribution function is:

$$f(\varepsilon) = \frac{1}{e^{(\varepsilon-\mu)/k_B T} - 1}. \quad (2.1)$$

At high temperatures, both this expression and its fermionic counterpart (identical except for a sign change in the denominator) reduce to the Boltzmann distribution. For bosons, as T approaches zero, the occupation of the lowest energy level of the system ($\varepsilon = 0$) can become macroscopically

large. When this happens, the sample undergoes a phase transition: a Bose-Einstein condensate forms. Because the particles in the BEC are all in a single quantum state (*i.e.* the ground state), they can be described by a single wavefunction. The constituent particles in a BEC can thus be likened to a ‘superatom,’ a system in which thousands or even millions of atoms behave like a single particle.

The phase transition can be understood in terms of the particles’ thermal de Broglie wavelength, λ_{dB} :

$$\lambda_{\text{dB}} = \sqrt{\frac{2\pi\hbar^2}{mk_B T}}, \quad (2.2)$$

where m is the mass of a particle. At high temperatures, the Heisenberg uncertainty principle dictates that the particles are well localised. As the temperature is reduced, the position uncertainty increases and the wave nature of the particles becomes more apparent. At sufficiently low temperatures, the de Broglie wavelength is long enough that the individual atomic wavefunctions overlap, and a condensate forms (Figure 2.1). The volume occupied by the atomic wave packets is multiplied by the peak number density of the sample to give the phase-space density, $PSD = n_{\text{pk}}\lambda_{\text{dB}}^3$. The transition to Bose-Einstein condensation occurs at a phase-space density of approximately 1.

To calculate the critical temperature T_c for the onset of BEC, we start by noting that it must occur when all N particles in the system can be ‘just barely’ accommodated in excited states, such that a further reduction in the temperature (kinetic energy) of the system leads to multiple occupation of the ground state. Under these conditions, the chemical potential is zero: any additional particles added to the system must go into the ground state, and the energy of the system does not change as a result of the addition¹. The total number of particles in the excited states N_{ex} can thus be written as

$$N_{\text{ex}}(T_c, \mu = 0) = N = \int_0^\infty g(\varepsilon) \frac{1}{e^{\varepsilon/k_B T_c} - 1} d\varepsilon, \quad (2.3)$$

where $g(\varepsilon)$ is the density of states. The form of $g(\varepsilon)$ depends on the potential (if any) in which the particles are confined. For our purposes, the most useful

¹We have assumed that N is large enough that we can neglect the zero-point energy.

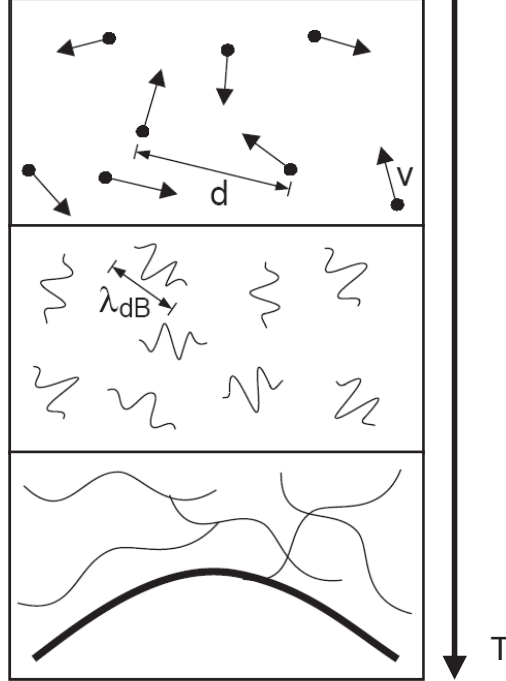


Figure 2.1: De Broglie wavelength and the transition to BEC. At temperatures $\gg T_c$ (top), the separation d between particles is much greater than their size, and atoms can be treated as point particles. As the sample is cooled (middle), the wave nature of the particles becomes more apparent. At $T \simeq T_c$, the individual atomic wavefunctions overlap, and a condensate forms (bottom). Figure adapted from [91].

potential to consider is that of a three-dimensional harmonic oscillator with cylindrical symmetry,

$$V(r) = \frac{1}{2}m\omega_r^2\rho^2, \quad (2.4)$$

which is approximately the potential generated by our magnetic trap. Here $\rho^2 = x^2 + y^2 + \lambda^2 z^2$ and $\lambda = \omega_z/\omega_r$ is the ratio between the axial and radial trap frequencies. The solution to Eq. 2.3 for this potential is [92]:

$$k_B T_c = \frac{\hbar\bar{\omega}N^{1/3}}{\zeta(3)^{1/3}} \simeq 0.94\hbar\bar{\omega}N^{1/3}, \quad (2.5)$$

where $\zeta(3)$ is the Riemann zeta function and $\bar{\omega} = (\omega_r^2\omega_z)^{1/3}$ is the average harmonic oscillator frequency. The transition temperature is thus higher

for large numbers of atoms confined in a tight trap, in accordance with the qualitative picture of wave packet overlap provided by our discussion of the particles' de Broglie wavelengths. For example, in the mixture experiment described in Chapters 4 and 5, we load Rb atoms into a trap for which $\omega_r/2\pi \simeq 11$ Hz and $\omega_z/2\pi \simeq 4$ Hz. At these trap frequencies, a sample of 10,000 atoms will reach degeneracy at a temperature of 7 nK. The same number of atoms in a trap with frequencies an order of magnitude higher would condense at 70 nK. Unfortunately, at higher densities, atoms are also more likely to be lost from the trap due to inelastic processes, *e.g.* three-body collisions. This is important, because as we shall see in the next section, the very diluteness of alkali condensates is an advantage in formulating theoretical descriptions of their behaviour.

2.2 An interacting gas

In the previous section, we considered Bose-Einstein condensation in purely thermodynamic terms as a quantum-statistical phase transition which occurs in the absence of interactions between particles. What happens if we want to include interactions? The usual method is to make the *mean-field approximation*, which allows interactions between all N particles in the gas to be described by a single interaction term H_{int} in the Hamiltonian [89]. For an interacting gas in an external potential V_{ext} , the mean-field Hamiltonian takes the form

$$H = H_0 + V_{\text{ext}} + H_{\text{int}}. \quad (2.6)$$

The mean-field approximation is often described alongside (and is sometimes equated with) the *Hartree approximation* [92], which allows us to write the wave function of an N -body system as the product of N single-particle wave functions. For a fully condensed sample, all bosons will be in the same single-particle state $\phi(\mathbf{r})$; hence we can write the condensate wave function Φ as

$$\Phi(\mathbf{r}_1, \mathbf{r}_2, \dots, \mathbf{r}_N) = \prod_{i=1}^N \phi(\mathbf{r}_i), \quad (2.7)$$

where the $\phi(\mathbf{r}_i)$ are *e.g.* the ground state wave functions of a harmonic oscillator, and are normalised to one. The *Bogoliubov approximation* assumes

that the non-condensate fraction of the system can be treated as a perturbation. This approach is used in more technical explanations of mean-field theory [89], where the Hamiltonian is initially written in terms of second-quantised field operators $\hat{\Psi}(\mathbf{r})$ and $\hat{\Psi}^\dagger(\mathbf{r})$, and then approximated to a form which includes only the condensate wave function Φ .

For some condensed systems, the mean-field treatment is a very bad approximation indeed, and breaks down on one or more of the conditions listed above. Interactions between superfluid helium atoms, for example, prevent more than $\sim 10\%$ of atoms from being the ground state even at temperatures very close to absolute zero [93]. The liquid nature of the helium system means that multi-body interactions and non-condensed fractions cannot be ignored or treated as perturbations, making helium condensates very difficult to describe theoretically.

In alkali gases like the mixtures of rubidium and caesium atoms which are the primary focus of this work, the interparticle separation is much greater than for He atoms in a superfluid. This does not mean that interparticle interactions in alkali gases are negligible. Indeed, some of the most fascinating phenomena in cold and ultracold atomic physics arise from interactions between particles. It is, however, often sufficient to consider only two-body interactions, for which theoretical treatments are comparatively tractable. For a low-energy, dilute gas, the interaction Hamiltonian H_{int} can be approximated by a contact potential (delta function) because the interparticle separation is usually much greater than the range of the attractive or repulsive forces between atoms [92]. At very low temperatures, the interactions between two identical bosons can be characterised by a single parameter: the s -wave scattering length a . This quantity is discussed in more detail in the next section. For the moment, we simply use it to write an expression for the Hamiltonian at low energies:

$$H = \sum_{i=1}^N \left(\frac{\hat{\mathbf{P}}_i^2}{2m} + V_{\text{ext}}(\hat{\mathbf{r}}_i) \right) + g \sum_{i<j} \delta(\hat{\mathbf{r}}_i - \hat{\mathbf{r}}_j), \quad (2.8)$$

where the coefficient of the interaction term g is defined as [92]

$$g = \frac{4\pi\hbar^2 a}{m}. \quad (2.9)$$

Using this Hamiltonian, we can write the well-known Gross-Pitaevskii equa-

tion (GPE) which describes the time-evolution of the trapped condensate:

$$i\hbar \frac{\partial}{\partial t} \Phi(\mathbf{r}, t) = \left(\frac{-\hbar^2}{2m} \nabla^2 + V_{\text{ext}}(\mathbf{r}) + g|\Phi(\mathbf{r}, t)|^2 \right) \Phi(\mathbf{r}, t), \quad (2.10)$$

where the number density $n(\mathbf{r}) = |\Phi(\mathbf{r}, t)|^2$. Again using the mean-field approximation, the condensate wave function $\Phi(\mathbf{r}, t)$ can be expressed as the product of a real part $\phi(\mathbf{r})$ and a time-dependent exponential $e^{-i\mu t/\hbar}$, where ϕ is normalised to the total number of atoms N . After minimising the energy of the system [92], we find the time-independent form of the GPE:

$$-\frac{\hbar^2}{2m} \nabla^2 \phi(\mathbf{r}) + V(\mathbf{r})\phi(\mathbf{r}) + g|\phi(\mathbf{r})|^2 \phi(\mathbf{r}) = \mu\phi(\mathbf{r}), \quad (2.11)$$

where μ is the chemical potential. These equations have the form of a non-linear Schrödinger equation, with the nonlinear term proportional to the number density and the scattering length. In the absence of interactions, Eq. 2.11 reduces to a linear Schrödinger equation. By contrast, the *Thomas-Fermi approximation* eliminates the kinetic energy term and concentrates on condensate behaviour due to the interactions (and external potential) alone. The conditions under which this approximation is valid are discussed in the next section.

2.3 Scattering theory

Quantum scattering theory is a well-established field with applications to a wide variety of physical systems. The purpose of this section is not to review scattering theory, but to define terms and introduce equations which are most necessary for understanding the role of scattering in cold and ultracold mixtures of rubidium and caesium. Detailed discussions of the aspects of scattering theory with greatest relevance for cold atomic gases may be found in numerous textbooks [92, 94–97] and theses [98–101].

The main scattering process of relevance for cold, dilute gases is two-body elastic scattering. Both evaporative and sympathetic cooling rely on elastic collisions between atoms to reduce the temperature of a sample. An unfavourable ratio of elastic (‘good’) collisions to inelastic (‘bad’) collisions has proved a serious stumbling block in efforts to cool some species of atoms,

notably caesium, to quantum degeneracy [68, 69]. The experimental apparatus described in this thesis was designed to study the collisional properties of a mixture of ^{87}Rb and ^{133}Cs , with an eye towards potentially overcoming the difficulties presented by cooling caesium alone. An understanding of the basic principles of elastic collisions is therefore essential.

2.3.1 Elastic scattering cross section

The Hamiltonian for the relative motion of two colliding atoms of mass m_1 and m_2 is

$$H = \frac{\mathbf{p}^2}{2M} + V(\mathbf{r}), \quad (2.12)$$

where $\mathbf{r} = \mathbf{r}_1 - \mathbf{r}_2$ and $\mathbf{p} = \mathbf{p}_1 - \mathbf{p}_2$, with $M = m_1 m_2 / (m_1 + m_2)$ being the reduced mass of the system. The eigenstates of this Hamiltonian with energy $E_k = \hbar^2 k^2 / 2M$ are the scattering states of the relative motion $\psi_{\mathbf{k}}(\mathbf{r})$. The solutions to the Schrödinger equation for this Hamiltonian take the form

$$\psi_{\mathbf{k}}(r) = e^{ikz} + f(\mathbf{k}) \frac{e^{ikr}}{r}, \quad (2.13)$$

where \mathbf{k} is the wave vector of the scattered wave, $f(\mathbf{k})$ is the scattering amplitude, and we have assumed that the potential vanishes as $r \rightarrow \infty$. The first term in Eq. 2.13 is an incoming plane wave, while the second is the scattered wave.

The scattering amplitude is related to the scattering cross section $\sigma(\mathbf{k})$ according to

$$\sigma(\mathbf{k}) = \int |f(\mathbf{k})|^2 d\Omega. \quad (2.14)$$

If we assume that the interaction between the atoms is spherically symmetric, we can write the scattering amplitude in terms of the scattering angle θ :

$$f(\theta) = \frac{1}{2ik} \sum_{l=0}^{\infty} (2l+1)(e^{i2\delta_l} - 1)P_l(\cos\theta). \quad (2.15)$$

Here, $l = 0, 1, 2, \dots$ denotes the contribution of s, p, d, \dots partial waves to the total scattering amplitude, δ_l are the phase shifts associated with each partial wave, and $P_l(\cos\theta)$ are Legendre polynomials. The full derivation of Eq. 2.15 can be found in Refs. [92] and [95]. Substituting this expression

into 2.14 and performing the integral over the full solid angle $0 \leq \theta \leq \pi$, $0 \leq \phi \leq 2\pi$ (ϕ being the azimuthal angle) yields

$$\sigma(k, \delta_l) = \frac{4\pi}{k^2} \sum_{l=0}^{\infty} (2l+1) \sin^2 \delta_l. \quad (2.16)$$

Up to this point, we have said very little about the properties of the particles being scattered, and have in fact assumed implicitly that they are distinguishable. If the particles are indistinguishable bosons (fermions), the ψ_k must be (anti)symmetric under interchange of the coordinates of the two particles, *i.e.* $\mathbf{r} \rightarrow -\mathbf{r}$, $\theta \rightarrow \pi - \theta$, $\phi \rightarrow \pi + \phi$. Taking into account the symmetries of the particles and the potential, Eq. 2.13 becomes

$$\psi_k = e^{ikz} \pm e^{-ikz} + (f(\theta) \pm f(\pi - \theta)) \frac{e^{ikr}}{r}, \quad (2.17)$$

where the plus sign applies to bosons and the minus sign to fermions. To find the scattering cross section for indistinguishable particles, we must change the limits of the integral in 2.14 to half the full solid angle to avoid double-counting. The result is a cross-section with *twice* the amplitude for classical particles,

$$\sigma(k, \delta_l) = \frac{8\pi}{k^2} \sum_{l=0}^{\infty} (2l+1) \sin^2 \delta_l. \quad (2.18)$$

Finally, it is worth noting that due to the $(-1)^l$ parity of the Legendre polynomials, the requirement that ψ_k be symmetric for identical bosons means that only even- l partial waves can contribute to the total scattering cross section. For fermions the reverse is true, and the suppression of s -wave scattering makes it impossible to achieve quantum degeneracy in single-species fermi gases. As discussed in the introduction, adding a second species reintroduces s -wave collisions to the system, and degeneracy of the target species is reached via sympathetic cooling with the second. A similar line of reasoning shows that although p -wave scattering is suppressed for single-species bosonic gases, this is not true for mixtures of two different bosonic species except at low temperatures. The next two subsections examine scattering in the limits of interest for our Rb-Cs system.

2.3.2 Low-energy elastic scattering

At low energies, the scattering cross section for bosons is dominated by the $l = 0$ term. This is because particles with nonzero angular momentum experience a centrifugal barrier in addition to the bare atom-atom interaction potential $V(r)$ [95]. If their relative kinetic energy is less than the barrier they never achieve interparticle separations where $V(r)$ is non-negligible, and scattering does not take place. For simplicity we will continue to approximate $V(r)$ as the contact interaction; for a discussion of scattering from other potentials, see *e.g.* Ref. [101]. In the $l = 0$ limit, Eq. 2.18 reduces to

$$\sigma = \frac{8\pi}{k^2} \sin^2 \delta. \quad (2.19)$$

It is often useful to express the phase shift in terms of an s -wave scattering length a . The relation between the two is [94]:

$$k \cot \delta = -\frac{1}{a} + \frac{1}{2} r_{\text{eff}} k^2 + O(k^4), \quad (2.20)$$

where the first-order correction term r_{eff} is known as the effective range. Setting this to zero for the moment, we can combine Eqs. 2.19 and 2.20 to write the scattering cross-section in terms of a :

$$\sigma = \frac{8\pi a^2}{1 + k^2 a^2}. \quad (2.21)$$

This relation has two important limits. For $ka \ll 1$, the scattering cross-section is $8\pi a^2$, equivalent to scattering from a hard sphere of radius a , and is independent of energy. When the modulus of the scattering length is much larger than the de Broglie wavelength of the scattered particles, *i.e.* $ka \gg 1$, the scattering cross-section reaches the *unitarity limit*, where

$$\sigma = \frac{8\pi}{k^2}. \quad (2.22)$$

In this regime, the scattering cross-section is independent of the scattering length. This state of affairs is associated with a phenomenon known as a *zero-energy resonance*. These resonances occur when the inter-atomic potential $V(r)$ is deep enough to support bound molecular states, and the energy of the last molecular bound state is close to the energy of the scattering state. When the depth of the potential is just less than the threshold for a new

bound state to appear, the scattering length is large and negative. If the potential depth is just higher than the threshold, the scattering length is large and positive [102]. The resonance occurs at the threshold, where a diverges.

The sign of the scattering length has important implications for the stability of Bose-Einstein condensates. For $a < 0$, the interaction between atoms is attractive, while for $a > 0$ it is repulsive. Attractive interactions lead to an increase in density at the centre of the condensed cloud, and for atom numbers above a critical value N_{cr} the kinetic energy of the atoms is no longer sufficient to prevent the condensate from collapsing [42]. In the case of repulsive interactions, the condensate is stable. In the limit that $Na/a_{\text{ho}} \gg 1$ (a_{ho} is the harmonic oscillator length $(\hbar/m\omega)^{1/2}$), we can make the Thomas-Fermi approximation, under which the interaction term in the GPE is assumed to dominate the condensate behaviour and the kinetic energy term is neglected. This greatly simplifies the form of the solutions to the GPE, which is especially important for mixed-species BECs [44, 45]. The implications of positive and negative scattering lengths for a mixture will be discussed later in this chapter.

What happens if we include the effective range correction? If we substitute Eq. 2.20 into Eq. 2.19, we find

$$\sigma = \frac{8\pi a^2}{k^2 a^2 + \left(\frac{1}{2}k^2 r_e a - 1\right)^2}. \quad (2.23)$$

The value of this approximation is that it is accurate even for large magnitudes of the scattering length, as discussed in Ref. [103] and shown graphically in Ref. [98]. This is particularly important for Cs, which in the $F = 3, m_F = \pm 3$ state has a scattering length with a magnitude of almost 3000 times the Bohr radius a_0 at zero magnetic field [74].

2.3.3 Higher partial waves

If the scattered atoms have a relative kinetic energy higher than the centrifugal potential barrier, the approximation that only s -wave collisions contribute to the total scattering cross-section is no longer valid. The form of

the centrifugal potential is [41, 94]

$$V_{\text{rep}} = \frac{\hbar^2 l(l+1)}{2Mr^2}. \quad (2.24)$$

Hence, the minimum energy required for higher- l partial waves to contribute is given by

$$E_l = \frac{\hbar^2 l(l+1)}{2M(R_{\text{min}})^2} - \frac{C_6}{(R_{\text{min}})^6}, \quad (2.25)$$

where C_6 is the van der Waals coefficient², M is the reduced mass and R_{min} is the radius at which the effective potential $\hbar^2 l(l+1)/(2Mr) - C_6/r^6$ reaches its maximum value, given by

$$(R_{\text{min}})^2 = \left(\frac{6MC_6}{\hbar^2 l(l+1)} \right)^{1/2}. \quad (2.26)$$

Figure 2.2 shows the van der Waals potential $-C_6/r^6$ and V_{rep} for $l = 1$ (solid blue line) and $l = 2$ (solid red line). The physical meaning of E_l and R_{min} is apparent from the sums of the two potentials (dashed lines).

For Rb-Rb and Cs-Cs scattering, the next allowed partial wave in the expansion is $l = 2$. Using the C_6 values found in Ref. [104], we see from Eq. 2.25 that the energy threshold at which d -wave scattering begins to contribute is approximately 420 μK for ^{87}Rb and 180 μK for Cs. To put these values into an experimental context, typical temperatures for Rb and Cs atoms in a well-optimised magneto-optical trap (MOT) are below 100 μK , while T_c for the alkali metals is typically measured in tens of nK. We will therefore treat the d -wave contribution to the scattering cross-section as negligible.

The threshold for p -wave scattering is lower, and for mixtures of two different bosonic species we have already noted that p -wave collisions are not suppressed as they are for a pure sample of Rb or Cs. Taking the value of the Rb-Cs C_6 from Ref. [105], we find that the threshold for p -wave scattering is approximately 56 μK — still well above the threshold for condensation, but cold enough to contribute in the MOT and during evaporative cooling in the magnetic trap. Table 2.1 contains a list of C_6 coefficients and scattering thresholds relevant to the Rb-Cs system.

²Literature values of the van der Waals coefficient are often given in atomic units. To convert into units appropriate for Eq. 2.25, one must multiply by a_0^6 and the Hartree energy $E_h = \hbar^2/(m_e a_0^2)$, where m_e is the electron rest mass and a_0 is the Bohr radius.

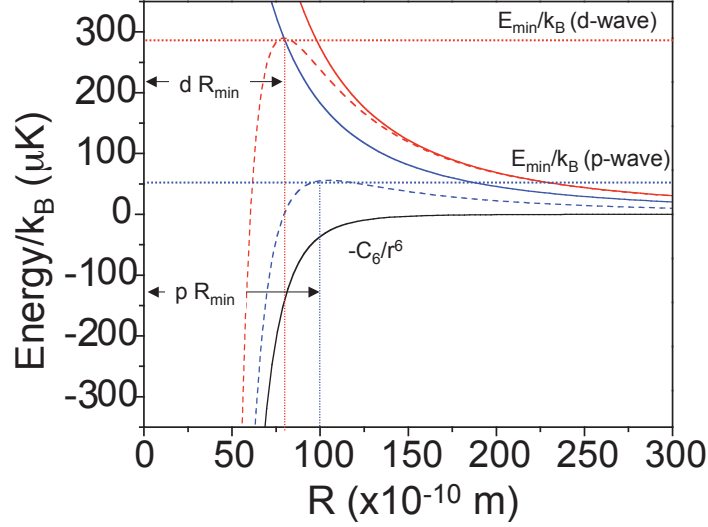


Figure 2.2: Scattering potentials for Rb-Cs. The solid black line indicates the van der Waals potential $-C_6/r^6$. Solid blue (red) lines show the potential barriers for p -wave (d -wave) scattering. Dashed lines indicate the sum of repulsive and attractive terms for p -wave (blue) and d -wave (red) scattering. The height of the potential barriers indicate that d -wave scattering will only occur at temperatures $\geq 290\mu\text{K}$, while the threshold for p -wave scattering is approximately $56\mu\text{K}$.

From Eq. 2.16, we find that the cross-section for s and p waves is:

$$\sigma_{s,p} = \frac{4\pi}{k^2} (\sin^2 \delta_0 + 3 \sin^2 \delta_1). \quad (2.27)$$

We can generalise our expression in Eq. 2.20 to account for higher partial waves, with the result that the scattering length for the l th partial wave is related to the scattering cross-section by

$$k^{2l+1} \cot \delta_l = -\frac{1}{a_l} + \frac{1}{2} r_l k^2 + O(k^4) \quad (2.28)$$

where we have substituted an l -dependent effective range for the earlier $l = 0$ value. Combining equations as before, we find that the cross-section for p -wave scattering is

$$\sigma_p = \frac{12\pi a_1^2 k^4}{1 + a_1^2 k^6}. \quad (2.29)$$

Note that this cross-section vanishes as $k \rightarrow 0$, as required.

	Rb-Rb	Cs-Cs	Rb-Cs
C_6	4691	6851	5284
p -wave	N/A	N/A	56 μ K
d -wave	410 μ K	180 μ K	290 μ K

Table 2.1: C_6 values (in atomic units) and scattering thresholds for the Rb-Cs system. Single-species C_6 values are taken from Ref. [104]; the Rb-Cs value is from Ref. [105].

2.4 Feshbach resonances

So far, we have treated atoms as structureless particles, for which only elastic collisions are possible. Inelastic collisions are more complicated, because the scattered atoms can be in different internal states – or, in the language of scattering theory, the incident and outgoing scattering channels are no longer the same, and multiple channels may contribute to the total scattering potential. Chapters 3 and 5 discuss inelastic collisions in the context of a two-species MOT, but for the moment, we will consider only one phenomenon associated with inelastic scattering: Feshbach resonances³.

As with zero-energy resonances, the change in scattering length near a Feshbach resonance occurs due to a coupling between the scattering state and the last bound state of the potential. For inelastic Feshbach resonances, the coupling occurs between the last bound state and *different* incoming and outgoing channels. For ground state atoms, these two channels are provided by different atomic hyperfine states. The energy of these states exhibits a magnetic field dependence via the Zeeman effect. By changing the magnetic field, a bound state supported by one scattering channel (closed channel) can be shifted into degeneracy with the scattering state of a second (lower energy) channel. This is illustrated in Figure 2.3. The result is that in the vicinity of a Feshbach resonance, the magnitude (and the sign) of the atoms' scattering length can be tuned over a wide range simply by changing the external magnetic field. The behaviour of the scattering length as a function

³Elastic Feshbach resonances are also possible, *e.g.* in the $|F = 3, m_F = +3\rangle$ state of Cs. For the purposes of this thesis and the related work described in Ref [84], we are primarily interested in inelastic resonances.

of the magnetic field B is given by

$$a(B) = a_{\text{bgd}} \left(1 - \frac{\Delta B}{B - B_{\text{res}}} \right), \quad (2.30)$$

where a_{bgd} is the scattering length far from resonance, ΔB is the width of the resonance and B_{res} is its position. The width of the resonance depends on the magnetic moment of the bound state and the coupling strength between the bound and scattering states.

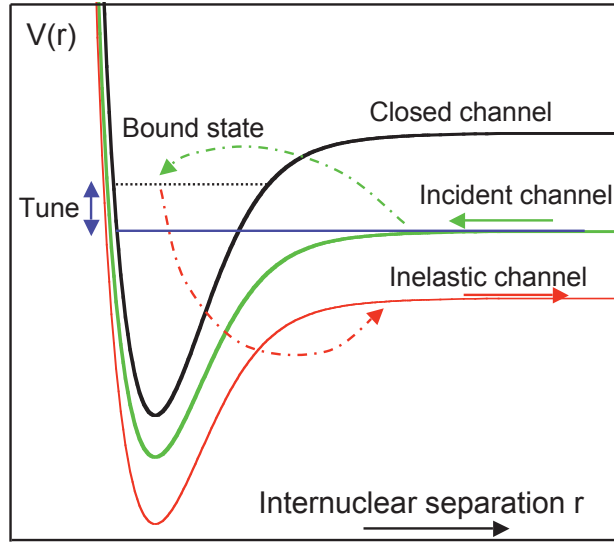


Figure 2.3: Illustration of scattering near an inelastic Feshbach resonance. Changing the magnetic field tunes the bound state supported by the closed channel into resonance with the incident channel, inducing a coupling to a lower-energy inelastic channel. Figure adapted from [98] and [106].

As the Gross-Pitaevskii equation (2.11) shows, changing the scattering length changes the strength of the interactions between the atoms. The importance of this tunability can hardly be overstated; indeed, Feshbach resonances have been compared to a ‘magic dial’ which would allow experimenters to alter the force of gravity at will! The tuneability of atomic interactions in the vicinity of a Feshbach resonance has been exploited experimentally for a number of purposes, including the creation of cold molecules [23] and solitons

[17, 18], the study of collapsing Bose-Einstein condensates [42], and investigations of the BEC-BCS crossover in fermionic systems [107–110]. They are also the subject of a rich theoretical literature (see, for example, Refs. [111–113]). The next section discusses their potential uses in a two-species mixture.

2.5 Two-species quantum degeneracy

To describe the behaviour of a two-species quantum degenerate gas using the mean-field approach, a second nonlinear term must be added to the Gross-Pitaevskii equations for the ground state of each species. The new term is proportional to the *interspecies* scattering length a_{12} , and represents interactions between the two species. The coupled equations are [44, 114]:

$$\begin{aligned} \left[-\frac{\hbar^2}{2m_1} + V_1(\mathbf{r}) + g_{11}|\psi_1|^2 + g_{12}|\psi_2|^2 \right] \psi_1 &= \mu_1 \psi_1 \\ \left[-\frac{\hbar^2}{2m_2} + V_2(\mathbf{r}) + g_{12}|\psi_1|^2 + g_{22}|\psi_2|^2 \right] \psi_2 &= \mu_2 \psi_2, \end{aligned} \quad (2.31)$$

where the coupling constants are defined as

$$\begin{aligned} g_{11} &= \frac{4\pi\hbar^2 a_{11}}{m_1} > 0 \\ g_{22} &= \frac{4\pi\hbar^2 a_{22}}{m_2} > 0 \\ g_{12} &= 2\pi\hbar^2 a_{12} \left(\frac{m_1 + m_2}{m_1 m_2} \right). \end{aligned} \quad (2.32)$$

The solutions to these coupled equations are discussed in many theoretical works; see, for example, Refs. [19, 44, 45, 114–116] and references therein. A number of factors dictate the form of the solutions. Firstly, there is the question of the relative separation of the two species, which is proportional to their trap frequencies and the gravitational acceleration g . If the two species have different masses (and, for magnetically-trapped mixtures, different magnetic moments), it is possible for the two condensates not to overlap at all, in which case the equations in 2.32 are no longer coupled.

Less trivial interaction regimes can be studied by examining the effects of different magnitudes and signs of each of the coupling constants on the

solutions. A useful parameter is the relative strength of the interactions Δ , which we define here as

$$\Delta = \frac{g_{12}}{\sqrt{g_{11}g_{22}}} \simeq \frac{a_{12}}{\sqrt{a_{11}a_{22}}}. \quad (2.33)$$

Note that a_{11} and a_{22} are assumed to be positive, for convenience [44].

2.5.1 Interaction regimes

The behaviour of the two-species quantum degenerate mixture for different values of Δ is illustrated in Figure 2.4. There are three distinct regimes of interest.

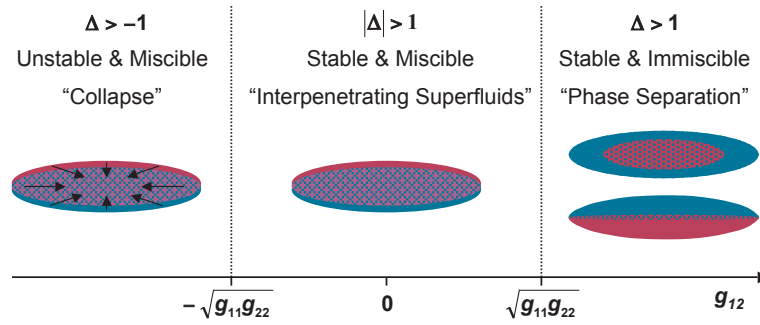


Figure 2.4: Behaviour of a two-species quantum degenerate gas at different relative interaction strengths.

Collapse

For $\Delta < -1$, the interspecies scattering length a_{12} is both negative and greater in magnitude than the geometric mean of the two single-species scattering lengths. In this case, the attractive interspecies interactions will dominate condensate behaviour, and lead to a collapse [19, 114]. Mathematically, the two BECs will only ‘overlap’ if there is a ‘hole’ in the condensate where both single-species wavefunctions vanish. This is not overlap in any physically meaningful sense.

Interpenetrating superfluids

For $|\Delta| < 1$, the interspecies scattering length may be either positive or negative, but its magnitude smaller than $\sqrt{a_{11}a_{22}}$. In this regime, the two condensates will be both stable and miscible. This is true even if the interspecies scattering length is negative, provided the restriction on the magnitude of $|\Delta|$ is not violated.

Phase separation

A final scenario occurs if $\Delta > 1$. In this case, a strong mutual repulsion leads to a phase separation between the two condensates. The ^{41}K - ^{87}Rb condensate first reported in Ref. [6] fell into this category.

2.5.2 Towards a tuneable mixture

In the previous section, we saw that Feshbach resonances allow the scattering length of a single-species cold gas to be tuned to a range of values simply by changing the magnetic field. For mixtures, one can perform experiments in which Feshbach resonances in one or both components of the two-species quantum degenerate gas allow Δ to be tuned between two or more regimes, facilitating the creation of heteronuclear cold molecules [23]. Interspecies Feshbach resonances, such as those described in Refs. [46–50] should allow even greater flexibility in tuning the value of Δ .